The relationship of volume and enthalpy changes in membranes studied for various chain lengths and headgroups by differential scanning calorimetry and pressure calorimetry

Katrine Rude Laub

March 8, 2010

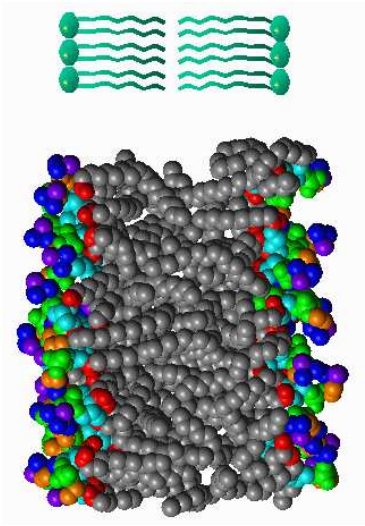

Bachelor project
University of Copenhagen
Niels Bohr Institute
Membrane Biophysics Group
Supervisor: Thomas Heimburg

Abstract

Statistical thermodynamics tells that the heat capacity is proportional to the fluctuations in enthalpy, and isothermal compressibility is proportional to the fluctuations in volume. Special for lipid membranes there seems to be a proportional relation between changes in enthalpy and volume near the chain melting transition. This means that simply by measuring the heat capacity one can get information about the compressibility. Compressibility is an interesting feature in relation to nerve pulses, cell division and other examples of structural changes.

This thesis discusses the proportionality between enthalpy and volume. The proportionality factor γ is determined for 8 different kinds of lipids by means of pressure calorimetry. It is found that γ is independent of the lipid, which means that compressibility easily can be determined even for unknown mixtures.

Changes in enthalpy during transitions are found by differential scanning calorimetry. A linear relationship between enthalpy change and chain length is found and discussed. Furthermore is given a description of the characteristic of the different lipid phases and transitions.

Frontpage: Two representations of a lipid bilayer. The picture is taken from www.tulane.edu/∼biochem/faculty/facfigs/bilayer.htm

This thesis is a bachelor project to 12.5 ECTS under Studieordning af 1997. The experiments described have been done in a period from September to December 2006 in the Membrane Biophysics Group, Niels Bohr Institute, University of Copenhagen.
The Danish title is: Forholdet mellem volumen- og enthalpiændringer i membraner undersøgt for forskellige kædelængder og hovedgrupper vha. differential scanning kalorimetri og trykkalorimetri.

Katrine Rude Laub

Contents

1 Introduction

This section contains some of the basic knowledge which is required to understand this project and put it into perspective. In the end of the section a motivation for the experiments are given.

1.1 Cells

Living organisms, from bacteria (unicellular) to human beings ($\sim 10^{14}$ cells), are made up of the same fundamental unit, the cell [1]. Many types of cells exist but all biological cells are surrounded by a membrane called the plasma membrane. This membrane serves as a semipermeable barrier that separates and protects the cell from its surrounding environment. The membrane is made of a double layer of lipids, mainly phospholipids, in which a variety of proteins are embedded. The proteins function among others as catalysts, channels and pumps that move molecules in and out of the cell.

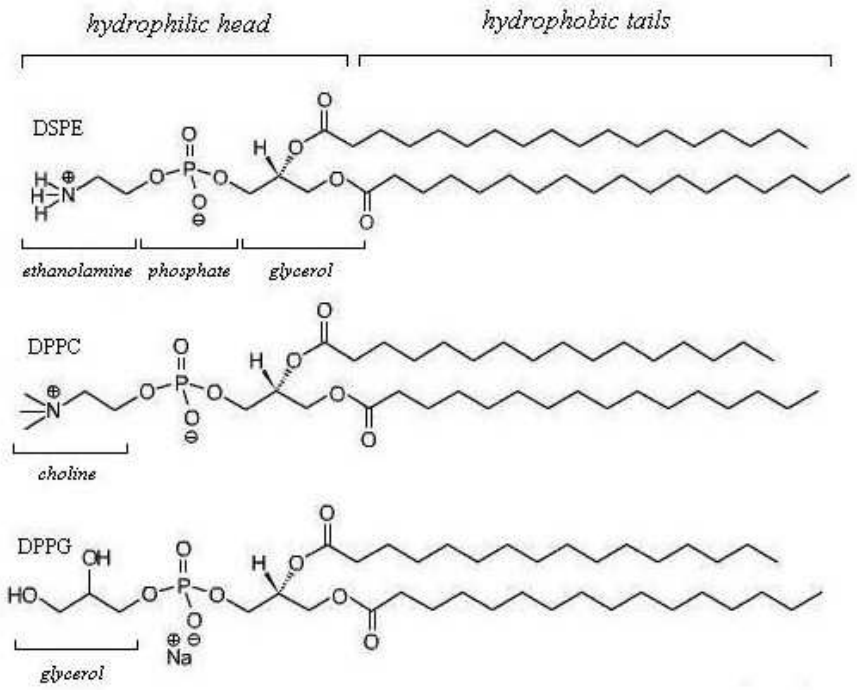

Figure 1: Structure of some phospholipids. Modified after [2]

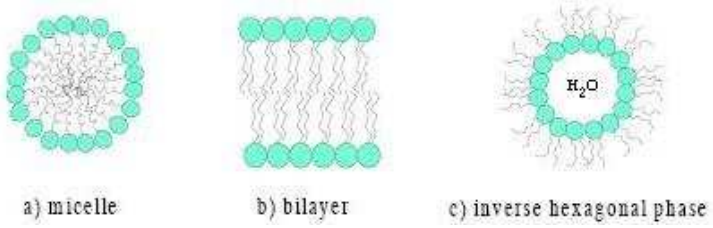

Figure 2: Structure of lipid aggregates [3]

1.2 Lipids and lipid membranes

A lipid is defined as a molecule that is soluble in organic solvent and insoluble in water [4]. Phospholipids are amphipathic molecules, i.e. molecules containing both a hydrophilic and a hydrophobic part (fig. 1). The hydrophilic part consists of the head group to which a tail of typically two hydrophobic hydrocarbon chains is attached. The carbon chains can vary in length and have different degrees of saturation i.e. number of double bonds.

When lipids are put into water they spontaneously aggregate in a way that minimizes the contact between the hydrophobic tails and water. The driving force of the self-assemble is the hydrophobic force, which can be seen as an entropic effect [5]. Strong hydrogen bonds exist between the water molecules. When a hydrophobic molecule is put into the water the bonds will not be disrupted but rather distorted. Thereby the water is forced to order around the hydrophobic molecule, forming a cage around it. This leads to a loss of configurationally entropy. When more hydrophobic molecules are present, more water molecules are confined to the cages. By pushing the hydrophobic molecules together the entropy can again be maximized.

Another effect holding the aggregates together is the rather weak van der Waals force. This force acts between neutral molecules and therefore primarily plays a role in the chain region. Van der Waals force arises from attraction between transient dipoles appearing because of uneven distributed electron densities around the molecules.

Different aggregate configurations are possible, but the far most important is the bilayer (fig. 2). This is the configuration used in all biological membranes. The thickness of a bilayer is approximately 5 nm [4, 6]. In order to avoid edges of the bilayer that bring the carbon chains in contact with water the bilayer can fold up into a vesicle, a small sphere with fluid inside and outside. The size of a vesicle can be between 25 nm and 1 μm in diameter depending on how they are produced [4]. At high lipid concentration more vesicles are formed inside each other [7]. The vesicles are said to be

multilamellar.

1.3 Motivation

Lipid membranes can undergo transitions accompanied by a significant change in heat capacity. It is found that the main transition temperature of biological membranes lies within a few degrees of physiological temperature [8]. If bacteria are grown at a lower temperature their membranes are altered in a way that gives them a lower transition temperature just below the one where they where grown. This indicates that organisms can make use of controllable factors such as pH and ionic strength to take the membranes in and out of transition and thereby gain advantage of the changes associated with the transition.

It is known from statistical thermodynamics that the heat capacity is proportional to the fluctuations in enthalpy, while isothermal compressibility is proportional to the fluctuations in volume. From this it follows that if enthalpy and volume are related functions, then their fluctuations are also related leading to a coupling between compressibility and heat capacity.

In lipid membranes there seems to be a simple proportionality between enthalpy and volume in the vicinity of the transition [14]. So by making simple calorimetric measurements of the heat capacity one can decide the compressibility. If the proportionality constant turns out to be the same for all lipids it becomes possible to deduce the compressibility of even complex lipid mixtures without knowing anything about their composition. Biomembranes have a very diverse mixture of lipids depending on where they function.

It is evident that structural changes related to compressibility do take place in transitions. Examples are the ripple phase and network formation in diacylphosphatidylglycerol which will both be described in the next section.

Change in compressibility is a relevant feature whenever structural changes shall take place. A biological example of such could be cell division. It is also found that a reversible change of temperature and heat accompanies nerve pulses. This leads to suggesting that the nerve signal is actually a propagating density pulse driven by the change in compressibility [9].

The goal of this thesis is to test if the proportional relation between enthalpy and volume changes exists. It will in addition be tried to find a possible relation between enthalpy and volume changes and the chain length in membranes for different types of lipids. The enthalpy change is measured with differential scanning calorimetry. Volume changes are measured with pressure calorimetry.

In this thesis I am only going to look at simple artificial membranes

Full name	Abbreviation	Chain length (C-atoms)	Molar weight (g/mol)
1,2-Dilauroyl-*sn*-Glycero-3-Phosphocholine	DLPC	12	621.84
1,2-Dimyristoyl-*sn*-Glycero-3-Phosphocholine	DMPC	14	677.94
1,2-Dipalmitoyl-*sn*-Glycero-3-Phosphocholine	DPPC	16	734.05
1,2-Distearoyl-*sn*-Glycero-3-Phosphocholine	DSPC	18	790.16
1,2-Dimyristoyl-*sn*-Glycero-3-Phosphoethanolamine	DMPE	14	635.86
1,2-Dipalmitoyl-*sn*-Glycero-3-Phosphoethanolamine	DPPE	16	691.97
1,2-Dimyristoyl-*sn*-Glycero-3-[Phospho-*rac*-(1-glycerol)]	DMPG	14	688.85
1,2-Dipalmitoyl-*sn*-Glycero-3-[Phospho-*rac*-(1-glycerol)]	DPPG	16	744.96

Table 1: List of lipids used in this project

consisting of one kind of saturated (no double bonds) phospholipid at a time. The lipids I use are listed in table 1. Note that the second letter in the abbreviation indicates the chain length and the last two letters indicate the type of headgroup.

2 Theory

2.1 Lipid phases and transitions

The different phospholipids show different peculiarities in their phase transitions. But they also have similarities. This section gives an overview of first the common phases and later of what characterizes the individual kinds of lipids. Finished theories do however not yet exist for all of them.

Four different, stable lipid phases exist. Ordered after increasing temperature the phases are: the crystalline phase, L_c, the solid ordered or gel phase, $L_{\beta'}$, the ripple phase, $P_{\beta'}$, and the liquid disordered or fluid phase, L_α [5, 10]. A schematic view on the lipid phases can be seen in fig. 3. Primes are used in the subscript when the chains are tilted.

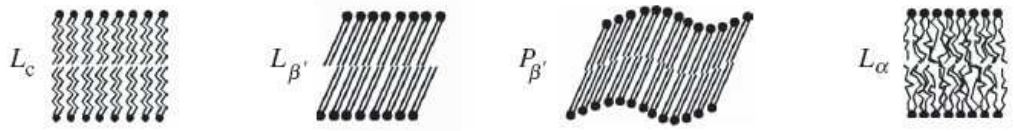

Figure 3: Lipid phases. From the left: crystalline, gel, ripple and fluid. Filled circles represent headgroups and lines are the chains. [11]

The L_c phase is characterized by being tightly packed and anhydrous. Rising temperature induces excitations where the lipids rotate around their long axis. This counteracts the van der Waals interaction between chains that favours the crystalline structure and the result is the $L_{\beta'}$ phase with a less tight packing and an increased hydration.

In $L_{\beta'}$ and L_α solid and liquid refer to the configurations of the headgroups, while ordered/disordered refer to the chains. In the solid state the headgroups are arranged in a triangular lattice structure. The liquid state can be seen as two-dimensional fluid, where the lipids can move freely in the plane of the bilayer.

With rising temperature the energy and entropy increase and more states become accessible. In saturated (only single bonds) lipids rotation around the C-C bonds is possible. Three stable conformations are found for the hydrocarbon chains: *trans, gauche*$^+$ and *gauche*$^-$ (fig. 4, *centre*). Because of steric interactions the energy of *gauche* is higher for *trans* (fig. 4, *right*). Kinks are the dominant kind of excitation in the melting regime [12].

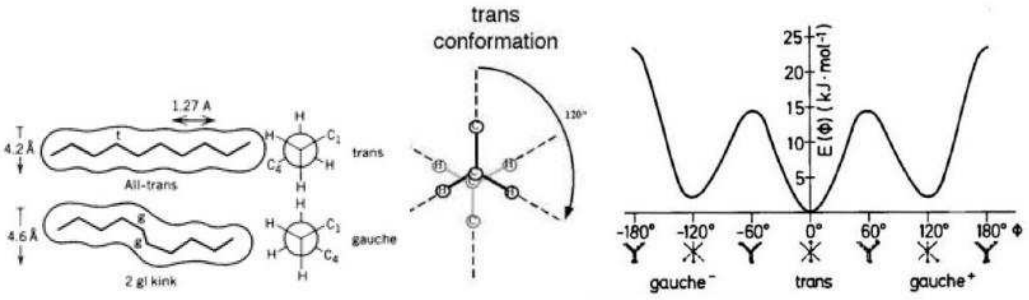

Figure 4: *Left:* Kinks arise from *gauche* conformations. *Centre:* A rotation of 120° of the chain around a C-C bond from the *trans* conformation gives a *gauche* conformation. *Right:* Energy as function of the angle between the hydrocarbon chains seen along a C-C bond. Figure taken from [15].

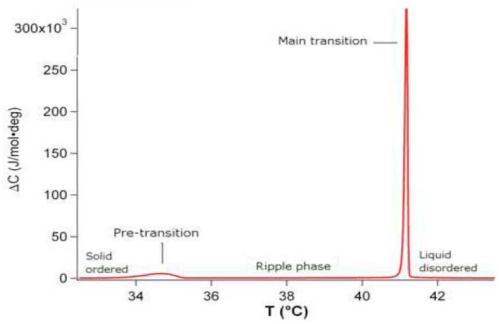

Figure 5: Heat capacity profile for DPPC [16]

At low temperatures the chains are all-trans and thereby parallel and fully extended. As the temperature rises the *gauche* conformation occurs more and more often. This creates the kinks (fig. 4, *left*) and the lipid melts.[1] The kinks make the packing less tight and the bilayer thinner (fig. 6B). The overall effect on the bilayer is an area expansion of 20-25% and an increase in volume of 4-5% from the gel to the fluid phase [5, 6, 13, 14].

Melting of lipids is a cooperative process. That means that the single lipid is influenced by its neighbours. An ordered lipid surrounded by disordered lipids has a higher probability of melting than one that is not. It is energetically unfavourable for single lipids to melt because of the difference in chain length between ordered and disordered lipids. To avoid exposure of hydrophobic parts lipids with the same length gather in domains [8, 16]. A high degree of cooperativity gives a narrow transition peak because the lipids melt at almost the same time.

The transition from L_c to $L_{\beta'}$ is named subtransition, between $L_{\beta'}$ and $P_{\beta'}$ it is called the pretransition, and the transition between $P_{\beta'}$ and L_α is the main transition (fig. 5). The distance between the pre- and the main transition depends on the chainlength [13, 17]. For PC it decreases with increasing length until the two transitions coincide for lipids with more than 20 carbon atoms.

Most of the melting takes place in the main transition. The melting temperature T_m is defined as the temperature where half the lipids are melted and the other half is not [6]. For biological lipids T_m lies in the regime -20 to +60 °C [6].

The ripple phase is an intermediate between the pre- and main transition and is named after its sawtooth-like surface, which has a periodicity in the

[1] Melting shall not only be understood as the colligative process of melting but also as the process where the single lipid creates kinks.

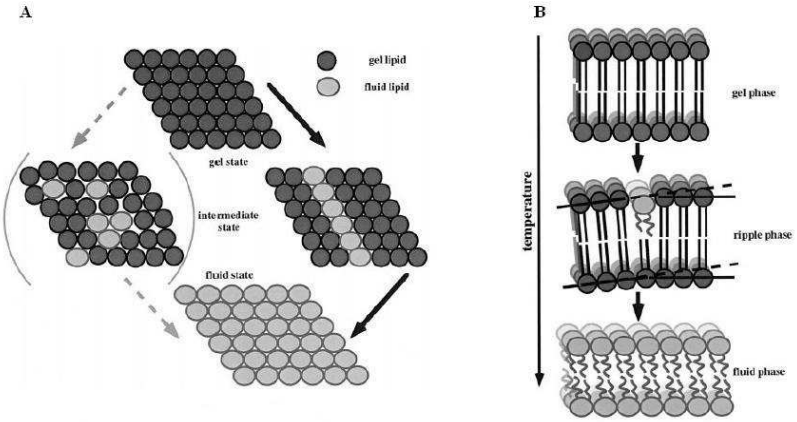

Figure 6: A: The triangular lattice during the melting process. B: The asymmetry induced by line defects cause local bending [13].

range of 100-300 Å [13]. In opposition both the gel and fluid phase is planar. One theory suggests that the ripples occur when disordered lipids face ordered lipids [13]. Individual, melted lipids disrupt the lattice because of their increase in area (see fig. 6A). The interactions between the lipids make it energetically favourable to keep the lattice structure and pack as tight as possible. Despite some of the lipids melting, it is possible to remain ordered. This can be done if instead of a random distribution, the melted lipids are arranged in lines along a lattice direction called line defects. A line defect induces curvature because of local area difference (fig. 6B), and a ripple is formed.

2.1.1 Diacylphosphatidylcholine (PC)

PCs are the standard example of the phases described above. However for chain lengths between 17 and 20 carbon atoms a new phase, the submain phase, appears [18]. The transition peak lies closer to the main transition with increasing chain length until 20 carbon atoms where they overlap. For the shorter chain lengths the transition might disappear in the calorimetric experiments because of decreasing enthalpy change with decreasing chain length.

Experiments with X-ray diffraction show that the submain transition occurs between two different ripple phases [19]. The corrugation remains but a rearrangement of the lipid packing (from an orthorhombic to a pseudo-hexagonal lattice structure) and a partial melting take place. The submain

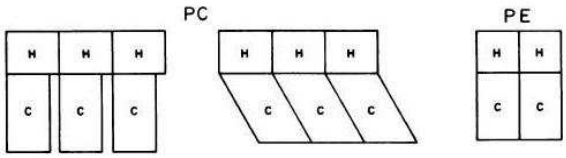

Figure 7: Schematic view of the packing of lipids. H represents the headgroup region and C the chain region. It is energetically favourable for the PC chains to tilt because of the excess space caused by the large headgroup. The smaller PE headgroup favours no tilt. [21]

transition has a very narrow peak and is the most cooperative transition observed in lipid bilayers [20].

DLPC is an exception from the other PCs I have used. For some reason it has a rather broad main transition peak similar to that of PGs which will be described later. I have not found any information of what is going on for DLPC.

2.1.2 Diacylphosphatidyletanolamine (PE)

Actually two versions of the gel phase exists: A tilted, $L_{\beta'}$, and one where the chains lies normal to the bilayer, L_β [17]. Which of the gel phases is seen depends on the headgroup. While PCs has the $L_{\beta'}$ version, L_β is seen in PEs.

The reason for the missing tilt shall be found in the size of the headgroup [21]. The headgroup of PCs ($\sim 50 \text{Å}^2$) has a larger area in the plane of the bilayer compared to the PEs' ($\sim 38 \text{Å}^2$) [22]. The larger area gives excess space for the chains, which tilts to increase the attractive van der Waals forces (fig. 7). In PEs the chains already fill out the space because of the smaller area, so a tilt serves no purpose.

The perpendicular chains might be related to the missing pretransition for PEs [23]. Lack of pretransition and normal chains seems to coincide [21], but exceptions can be found [24].

The gel phase of PEs is found to be metastable [5, 26, 27, 28]. It spontaneously reverses into a less hydrated and more ordered phase resembling the crystalline phase if kept at low temperature for enough time. It is assumed that the unfavourable dehydration is more than compensated by increased van der Waals interactions in the tightly packed chains [5, 27]. For some reason the reversion is normally not to the normal L_c form but to a $L_{c'}$ form with tilted chains. For DLPE it is reported that the $L_{c'}$ form has a melting

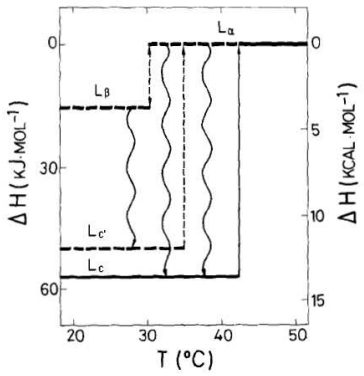

Figure 8: Schematic representation of the various phases in DLPE. Stable phases and transitions are illustrated by unbroken lines. Metastable phases and transitions are illustrated by dashed lines. The wavy lines illustrate time dependent transitions at constant temperature [27].

point lower than L_c ($T_m(L_c)$) but higher than the melting point of the hydrated gel phase $T_m(L_\beta)$. This means that when incubated at a temperature T where $T_m\,(L_\beta) < T < T_m\,(L_c)$ the fluid hydrocarbon chains may spontaneously crystallize to the L_c form [5, 27]. Fig. 8 gives a representation of what just described.

When first heated to above $T_m\,(L_c)$ the lipid is hydrated and returns to the hydrated gel phase by cooling. The anhydrous phase can be restored after prolonged storing at low temperature [25].

2.1.3 Diacylphosphatidylglycerol (PG)

DMPG turns out to have a rather broad main transition starting at T_m^{on} and ending at T_m^{off} (see fig.). Exactly what courses this shape of the transition is subject to several theories. What seems to be sure is that below T_m^{on} the lipid is in a gel phase and it is not fluid before above T_m^{off} [29]. In between a new intermediate phase (IP) appears with a significantly increased viscosity [30].

It is also well established that curvature broadens the melting transition [31]. In [22] this is used to explain the broad melting regime in PG vesicles. PGs have effectively larger headgroups than PEs and PCs. This is partly because it is geometrically large ($\sim$44Å^2) compared to cross section of the chains and partly due electrostatic repulsion between the anionic heads. The large headgroups gives a higher curvature of the vesicles (fig. 9). This results in a looser packing of the chains (compare fig. 9 A and C), which diminishes

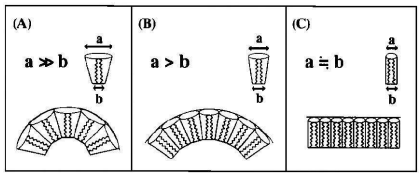

Figure 9: Packing of lipids depends on the cross sectional area of the headgroup (a) compared to the chains (b), which are here held constant. A large headgroup gives a high curvature [22].

the cooperativity and thereby gives a broader melting region.

A way of avoiding the broad melting regime is addition of NaCl [22, 30]. The ions provide a screening effect between the heads, whereby the curvature decreases. In addition increasing NaCl concentrations, increase the multiplicity of bilayers (the vesicles become multilamellar) [22]. PG vesicles in dispersions of low ionic strength are unilamellar because of electrostatic repulsion between the charged PGs in multilamellar vesicles [22, 32].

The increased viscosity in the IP has been explained by [30] to be the effect of formation of a 3-dimensional membrane network (fig. 10, *left*). Large facetted vesicles has been observed that below T_m^{on} and smaller spherical vesicles above T_m^{off}. This leads to suggesting that interactions with the solvent favours the curvature found in a long range network. It is in addition found that decreasing chain length gives broadening of the melting regime. For DPPG only a single peak is observed.

Other experiments suggest that the theory of a 3-dimensional network does not hold. In [29] it is described how DMPG suspensions have been tested for fusion of vesicles. It is found than no fusion takes place and therefore networks can not be formed. At high lipid concentrations (>70mM) however there might anyway be a destruction of vesicles in the IP [32].

It is instead suggested that in the IP networks of fissures and perforations with highly curved edges arise in the normal bilayer vesicle (fig. 10, *right*). The onset of chain melting gives rise to separation of the lipids due to electrostatic repulsion of the heads. Thereby water is allowed to penetrate the membrane and perforations are created. In the figure the vesicle surface is shown to be smooth in the IP. This is probably not the case as the curvature defects presumably change the vesicle topology.

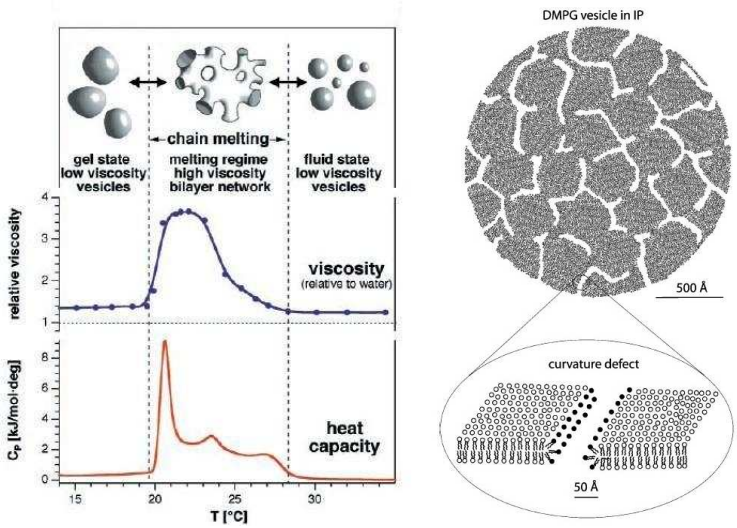

Figure 10: Theories for the structure of the intermediate phase (IP) in DMPG. *Left:* Profiles of heat capacity and viscosity coupled to the formation of a 3-dimensional network structure [30]. *Right:* Fissures in the bilayer creates a 2-dimensional network in the vesicle surface [32].

2.2 Themodynamics

This section gives the thermodynamic background for the experiments[2]. First is given a reminder of some of the basic thermodynamic equations.

2.2.1 Basics

In the following U denotes internal energy, S is the entropy, V the volume, T the temperature and p is the pressure.

The partition function, Z, is a summation over the Boltzmann factor, $\exp(-\varepsilon_s/k_BT)$, for all states, s, of the system. ε_s is the energy of the state s.

$$Z(T) = \sum_s \exp(-\varepsilon_s/k_BT) \tag{1}$$

The average, $\langle X \rangle$, of a distribution is given by

[2]Sections 2.2.1 and 2.2.2 is inspired of [33] and sections 2.2.3 and ??is inspired of [14] and [34]

$$\langle X \rangle = \sum_s X(s) P(s) \tag{2}$$

where $P(s)$ is a probability assigned to each state of the system. It is given that $P(s)$ is normalized to unity. The partition function is the proportionality factor connecting the probability and the Boltzmann factor.

$$P(\varepsilon_s) = \frac{\exp(-\varepsilon_s / k_B T)}{Z} \tag{3}$$

In terms of the partition function is the average then given as

$$\langle X \rangle = \sum_s \frac{X_s \exp(-\varepsilon_s / k_B T)}{Z} \tag{4}$$

Enthalpy, H, is defined as

$$H = U + pV \tag{5}$$

From this it is given

$$dH = dU + pdV + Vdp \tag{6}$$

Heat capacity at constant pressure, c_p, is given by

$$c_p = T \left(\frac{\partial S}{\partial T} \right)_p \tag{7}$$

A useful relation is the thermodynamic identity

$$dU = TdS - pdV \tag{8}$$

By a reversible change of state TdS can be identified as the heat, dQ, added to the system and $-pdV$ as the work, dW, done on the system.

2.2.2 Differential scanning calorimetry

If you put eqn. 8 into eqn. 7, use eqn. 6 and remember that the pressure is constant you get

$$c_p = \left(\frac{\partial U}{\partial T} \right)_p + p \left(\frac{\partial V}{\partial T} \right)_p = \left(\frac{\partial H}{\partial T} \right)_p \tag{9}$$

From this it is seen that the enthalpy can be calculated by integrating the heat capacity.

$$H = \int_{T_1}^{T_2} c_p dT \tag{10}$$

This equation will be used when handling the calorimetric data.

2.2.3 Pressure calorimetry

In the following the relation between melting temperatures at different pressures is found.

In an ensemble of lipids the mean enthalpy change, $\langle \Delta H \rangle$ is (cf. eqn. 4)

$$\langle \Delta H \rangle = \frac{\sum\limits_s \Delta H_s \exp\left(-\Delta H_s / k_B T\right)}{\sum\limits_s \exp\left(-\Delta H_s / k_B T\right)} \tag{11}$$

For each microstate, i, at pressure p_0 the enthalpy is given by (cf. eqn. 5)

$$\Delta H_i^0 = \Delta U_i + p_0 \Delta V_i \tag{12}$$

At a different pressure $p_0 + \Delta p$ it is

$$\Delta H_i^{\Delta p} = \Delta U_i + \left(p_0 + \Delta p\right) \Delta V \tag{13}$$

Experiments have suggested that at a given temperature the mean enthalpy and volume changes are proportional functions[3] [14, 34].

$$\langle \Delta V \rangle_T = \gamma \langle \Delta H \rangle_T^0 \tag{14}$$

This also holds for each microstate.

$$\Delta V_i = \gamma \Delta H_i^0 \tag{15}$$

The relation is in the following assumed to be true. It then follows from eqn. 12-15 that

$$\begin{aligned} \Delta H_i^{\Delta p} &= \Delta U_i + p_0 \Delta V_i + \Delta p \Delta V_i \\ &= \Delta U_i + p_0 \Delta V_i + \gamma \Delta p \Delta H_i^0 \\ &= \Delta H_i^0 \left(1 + \gamma \Delta p\right) \end{aligned} \tag{16}$$

From eqn. 11 and the above the mean enthalpy at pressure $p_0 + \Delta p$ is

[3] Lipids where this relation does not hold can be found. An example is PGs in a solvent of low ionic strength [30].

$$\begin{aligned}\left\langle \Delta H_T^{\Delta p} \right\rangle &= (1+\gamma\Delta p)\frac{\sum_i \Delta H_i^0 \exp\left(-(1+\gamma\Delta p)\,\Delta H_i^0/k_BT\right)}{\sum_i \exp\left(-\left(1+\gamma\Delta p\right)\Delta H_i^0/k_BT\right)} \\ &= (1+\gamma\Delta p)\frac{\sum_i \Delta H_i^0 \exp\left(-\Delta H_i^0/k_BT^*\right)}{\sum_i \exp\left(-\Delta H_i^0/k_BT^*\right)} \end{aligned} \tag{17}$$

In the last equation the rescaled temperature, T^* has been introduced

$$T^* = \frac{T}{1+\gamma\Delta p} \tag{18}$$

From this the proportionality constant, γ, can be calculated and then used to determine the volume change using eqn. 15.

It is furthermore seen that the mean enthalpy change at two different pressures is proportional when using T^*

$$\langle \Delta H \rangle_T^{\Delta p} = (1+\gamma\Delta p)\,\langle \Delta H \rangle_{T^*}^0 \tag{19}$$

It follows that after rescaling of the temperature axis using eqn. 18 the two curves made at different pressures should have the same shape. If this is not the case the assumption in eqn. 15 is not true.

2.2.4 Compresibility

Differentiation of $\langle \Delta H \rangle$ with respect to temperature gives

$$\begin{aligned}\frac{\partial \langle \Delta H \rangle}{\partial T} &= \frac{\sum_i \frac{\partial \Delta H_i}{\partial T}\exp\left(-\Delta H_i/k_BT\right)}{\sum_i \exp\left(-\Delta H_i/k_BT\right)} + \frac{\sum_i \left(\Delta H_i\right)^2 \exp\left(-\Delta H_i/k_BT\right)}{\sum_i \exp\left(-\Delta H_i/k_BT\right) k_BT^2} \\ &- \frac{\left[\sum_i \Delta H_i \exp\left(-\Delta H_i/k_BT\right)\right]^2}{\left[\sum_i \exp\left(-\Delta H_i/k_BT\right)\right]^2 k_BT^2} \\ &= \frac{\langle \Delta H^2 \rangle - \langle \Delta H \rangle^2}{k_BT^2} \qquad (20) \\ &= \frac{\left\langle \left(\Delta H - \langle \Delta H \rangle\right)^2 \right\rangle}{k_BT^2} \qquad (21)\end{aligned}$$

The first term after the equality disappears because ΔH_i is constant. It can now be seen that the fluctuations in the enthalpy is proportional to the heat capacity (cf. eqn. 9) .

$$c_p = \frac{\left\langle (H - \langle H \rangle)^2 \right\rangle}{k_B T^2} \tag{22}$$

It is furthermore seen that c_p is always positive in an equilibrium system. The mean value of the volume change is

$$\Delta\kappa_T = -\frac{1}{\langle \Delta V \rangle} \left(\frac{\partial \langle \Delta V \rangle}{\partial p} \right)_T = \frac{\langle \Delta V^2 \rangle - \langle \Delta V \rangle^2}{\langle \Delta V \rangle k_B T} \tag{23}$$

By inserting eqn. 6, assuming the pressure is constant and differentiating with respect to p one gets

$$\frac{\partial \langle \Delta V \rangle}{\partial p} = \frac{-\langle \Delta V^2 \rangle + \langle \Delta V \rangle^2}{k_B T} \tag{24}$$

The change in isothermal compressibility, $\Delta\kappa_T$, is defined as

$$\Delta\kappa_T = -\frac{1}{\langle V \rangle} \left(\frac{\partial \langle \Delta V \rangle}{\partial p} \right)_T = \frac{\langle \Delta V^2 \rangle - \langle \Delta V \rangle^2}{\langle V \rangle k_B T} \tag{25}$$

Using eqn. 15 it can now be seen that the compressibility can be related to the heat capacity.

$$\Delta\kappa_T (T) = \frac{\gamma^2 \left(\langle \Delta H^2 \rangle - \langle \Delta H \rangle^2 \right)}{\langle V (T) \rangle k_B T} = \frac{\gamma^2 T}{\langle V \rangle} \Delta c_p \tag{26}$$

This means that with knowledge about the heat capacity, which is easily measured, it is possible to calculate the compressibility in even complex lipid mixtures.

2.2.5 Transition temperature

Latent heat, L, of a phase transformation at constant pressure is equal to T times the change of entropy between the two phases.

$$L = T\Delta S \tag{27}$$

L is also equal to the change in enthalpy

$$L = T\Delta S = \Delta U + p\Delta V = \Delta H \tag{28}$$

The second equality comes from eqn. 8 and the third from eqn. 6. From this it is seen that the transition temperature, T_t is equal to the change in enthalpy divided by the change in entropy.

$$T_t = \frac{\Delta H_t}{\Delta S_t} \tag{29}$$

This is an alternative way of defining the transition temperature [10].

3 Materials and methods

For calculation of the concentration c the following equations are used

$$n = c \cdot V \qquad \text{and} \qquad m = n \cdot M \tag{30}$$

Here V denotes the volume, n the amount of moles, m the mass and M the molar weight.

3.1 Buffer

In order to keep the conditions constant the lipids are diluted in a buffer containing water[4], 10 mM Hepes (purchased from Sigma-Aldrich, St. Louis/MO, USA) and 1 mM EDTA (from Fluka, Buchs, Switzerland).

Hepes (4-(2-hydroxyethyl)-1-piperazineethanesulfonic acid) is used to keep the pH steady. EDTA (ethylenedinitrilotetraacetic acid) is used to prevent growth of bacteria. EDTA binds calcium, which bacteria require.

The masses of Hepes and EDTA was calculated using eqn. 30. The pH was afterwards set to approximately 7 by adding NaOH and HCl until the desired pH was achieved. This has a slight influence on the concentrations of Hepes and EDTA, but because the amounts added are small compared to the volume of the buffer and the concentrations are not used anywhere in the calculations, this is of no importance.

3.2 Sample preparation

The lipids are purchased from Avanti Polar Lipids (Alabaster/AL, USA) and used without further purification.

All lipid solutions are made with concentration of 68.5 mM. A high concentration is used to diminish the effect of uncertainties in the preparations.

[4]The PC are diluted in a buffer based on demineralised water, while the other lipids are diluted in a buffer based on Millipore water. Millipore water is demineralised water from which also ions have been removed

The mass needed for the given concentration is calculated from eqn. 30. The lipids where weighed within an error of ± 0.001g and the needed volume of buffer was added within an error of 1%. Afterwards the solution was heated to above the expected melting temperature and stirred by a magnetic stirrer until the solution became homogeneous. The samples where stored by a temperature of -22 °C when not in use.

The melting point of DLPC is placed at a temperature close to 0°C. A solution normally has a lower freezing point than a pure solvent, so in order to avoid that the buffer freezes during the measurements, glycerol is added. The freezing temperature of a solution is found as the freezing temperature of the pure solvent minus ΔT_m, where ΔT_m is given as

$$\Delta T_m = E_f \cdot c_m \tag{31}$$

where E_f is the freezing point depression constant (or cryoscopic constant) and c_m is the molal concentration, i.e. the amount of moles solute per kilogram of solvent.

To the PGs was added NaCl. The concentration in the DPPG-solution was 554 mM and in the DMPG it was 674 mM. To comparison a solution with DMPG and without NaCl was also made.

3.3 Instruments

3.3.1 Differential scanning calorimetry

The differential scanning calorimeter (DSC) is used to measure the heat capacity during phase transitions. The calorimeter used is of the type VP-DSC produced by Microcal (Northhampton/MA, USA) and operated using a computer.

The DSC consists of two cells with capillaries in an adiabatic box isolated from surroundings (fig. 11 *left*). Measurements are done only on the cells. One cell contains the sample and the other one is the reference, which in this case is buffer. The calorimeter is in my experiments filled only to the edge of the cell. This is to avoid a change in concentration of the sample caused by sinking of the lipids during the experiments. The calorimeter is filled using a high-precision syringe with a volume equal to the cell volume of 0.5152 mL.

The DSC can be set to continuously change the temperature T of the cells and meanwhile maintain the temperature difference between the cells equal to zero. The excess power ΔP added to the sample cell compared to

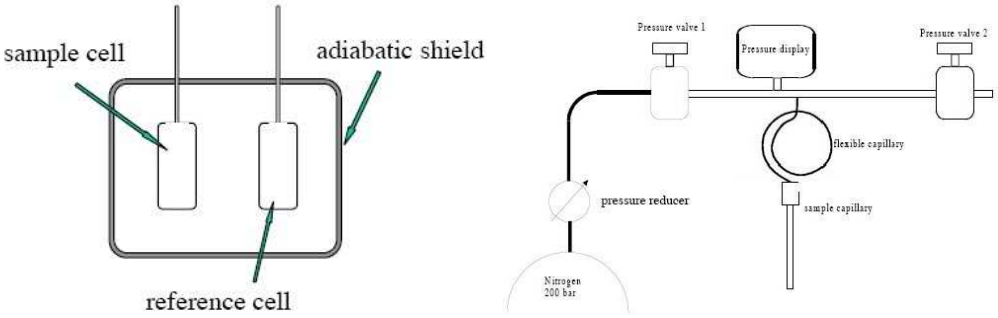

Figure 11: *Left:* Construction of the differential scanning calorimeter. *Right:* Setup for pressure calorimetry. [3]

the reference cell is then recorded. The excess heat ΔQ is then found by integration of the excess power with respect to time t.

$$\Delta Q = \int_t^{t+\Delta t} \Delta P\,(t')\,dt' \simeq \Delta P \cdot \Delta t \tag{32}$$

At constant pressure and volume the (excess) heat capacity C_p is given by (cf. eqn 9 and 8)

$$C_p = \left(\frac{\partial Q}{\partial T}\right)_p \simeq \left(\frac{\Delta Q}{\Delta T}\right)_p = \frac{\Delta P}{\frac{\Delta T}{\Delta t}} \tag{33}$$

where $\frac{\Delta T}{\Delta t}$ is the scan rate. I have used a scan rate of 2°C/hr during most of the experiments. It is important with a low scan rate so that every step happens via equilibrium states. The scans are done in intervals approximately 10°C below the expected pretransition temperature and 10°C above the expected main transition temperature. For most samples has been made both a heating and a cooling scan to see if the process is reversible.

3.3.2 Pressure calorimetry

For pressure calorimetry is used the setup shown in fig. 11, *right*. Instead of putting the sample directly in the sample cell it is put in the sample capillary. The capillary is connected to a nitrogen container that provides the pressure. During the measurement the pressure is enclosed between the two valves. The barometer is set to zero at atmospheric pressure. Pressures between 150 and 165 bar have been used and it is displayed with an accuracy of 0.1 bar. In some measurements the pressure has fallen a few bars during

the scan. In these cases an average of the pressure before and after is used for the calculations.

The capillary is placed in the sample cell surrounded by water to ensure a continuous flow of heat to the capillary. To avoid evaporation the opening in the calorimeter was closed by wrapping parafilm around it. A normal DSC-scan is performed. For time reasons only heating scans have been made with this technique for most of the samples.

3.4 General considerations

All equipment used have been cleaned carefully with water and ethanol and dried with nitrogen. The capillary used in the pressure experiment have been kept in vacuum for at least an hour to make sure no ethanol resided in the bottom. Buffer and lipid solutions have been under compression for 15 minutes before placed in the calorimeter to remove bubbles.

3.5 Handling the data

The data output is collected in a file, which is analyzed with the graphics program Igor Pro 5.03 (Wavemetrics). Before integrating over the transition peaks one has to subtract a baseline in order to get the excess power outside the transition regime to approach zero. In this way only the heat capacity of the transition comes out. It is done by cut out the transition data and fit the remaining data to a polynomial. It can be a rather subjective judgment to decide how much to cut out and which polynomial gives the best fit and thereafter decide the range over which integration shall be done. For this reason I have done the procedure 10 times for each lipid when calculating the enthalpies. In the worst cases I get a standard deviation of up to 7% but generally it lies between 2% and 5%.

4 Results

4.1 Heat capacity profiles

PC

Fig. 12, *left* shows the heat capacity profiles of the four PCs tested. It is seen that the transition temperature rises and that the pre- and main transition gets closer with increasing chain length. A broad transition regime is observed for the short chained DLPC. In the profile of DSPC the submain transition is clearly seen.

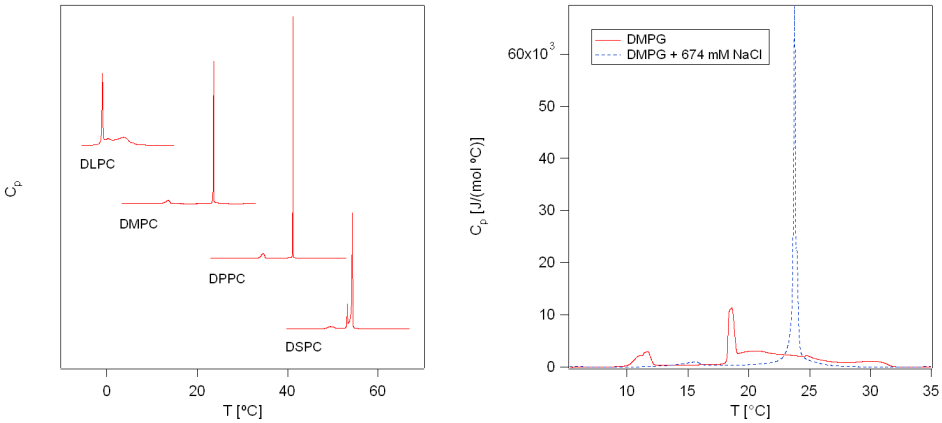

Figure 12: Heat capacity profiles of PCs (*left*) and DMPG with and without addition of NaCl (*rigth*). The heat capacity of DLPC has been rescaled with a factor 5.

PG

DMPG has a broad transition regime, which become narrowed by addition of NaCl (fig. 12, *right*). The enthalpies found for DMPG with and without NaCl are respectively 23.2 kJ and 24.8 kJ for the main transition and 28.3 kJ and 31.3 kJ for the pre and maintransition. So addition of NaCl might alter the transition enthalpy a bit, but the broad transition without NaCl makes it more difficult to decide exactly where it begins and ends. In addition I did not have much baseline in NaCl missing heat capacity profile to make the polynomial fit from. This gives a greater uncertainty.

PE

Fig. 13 shows consecutive scans of a DMPE sample which has not been heated to above melting temperature during preparation. The experiment has been repeated on two different samples with the same result. There seems to be an occurrence of non-equilibrium, which I will go deeper into in the discussion section. No pretransition is seen in any scan on PEs. The curves C and E have been used when determining the enthalpy.

Enthalpy dependence of chain length

The transition enthalpies of each lipid type can be seen in fig. 14 as a function of chain length, n. Enthalpies for both the main transition and the main plus the pretransition are given. This is because the melting might start already

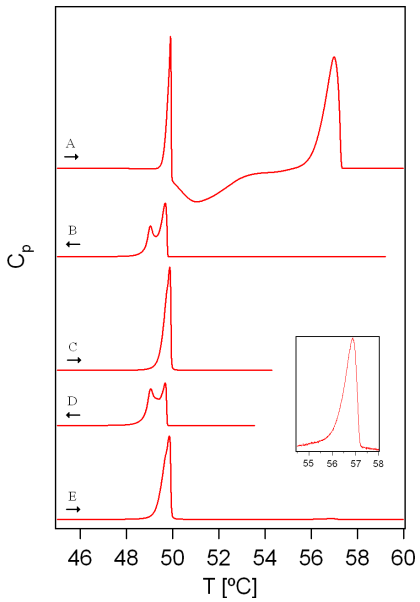

Figure 13: Heat capacity profiles of DMPE made consecutively from A to E. Right arrows indicate heating scans and left arrows indicate cooling scans. Horizontal lines represent zeros. Insert is a blow up of E.

in the ripple phase as described in section 2.1. I have not measured at low enough temperatures to see the pretransition of DLPC. For representing the PGs I have used the enthalpy for DMPG added NaCl because I only have measured the enthalpy of DPPG with addition of NaCl. Enthalpies of submain transitions are included in the numbers used in the graph.

4.2 Pressure calorimetry

Some examples of pressure calorimetry experiments are given in fig. 15. It can be seen that application of pressure shifts the transition to a higher temperature. The rescaling factor for temperature (cf. eqn. 18) have been found for each sample in order to decide the proportionality factor γ. The results are given in table 2. The average of γ is found to be $7.72 \cdot 10^{-4} \pm 0.22 \cdot 10^{-4}$ml/J. The average value found in [14] is $7.79 \cdot 10^{-4}$ ml/J which within error is the same as the one I have determined.

For some reason I in general do not get very good matches between the low pressure sample and the rescaled high pressure sample after rescaling. Only for a couple of lipids I get an almost exact match. For the others the shapes are similar but in some cases the high-pressure curves are a bit wider

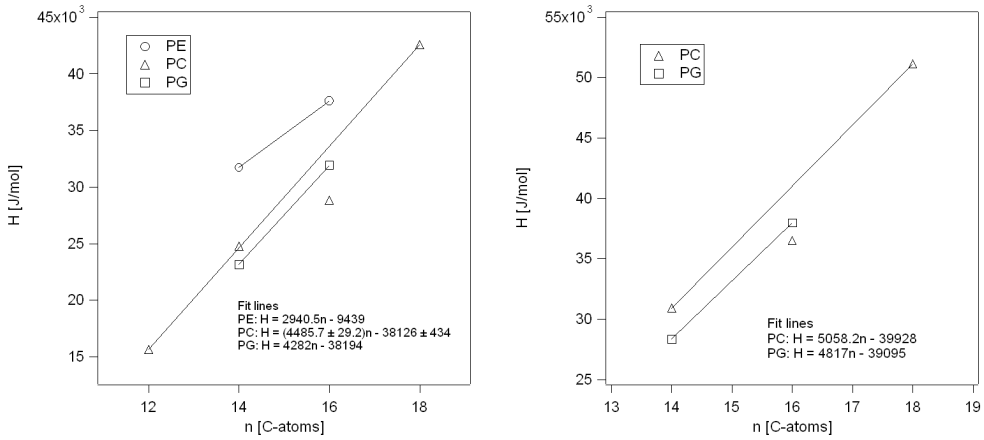

Figure 14: *Left:* Enthalpies of the main transition as a function of chain length. *Right:* Enthalpies of the pre- and main transition as a function of chain length.

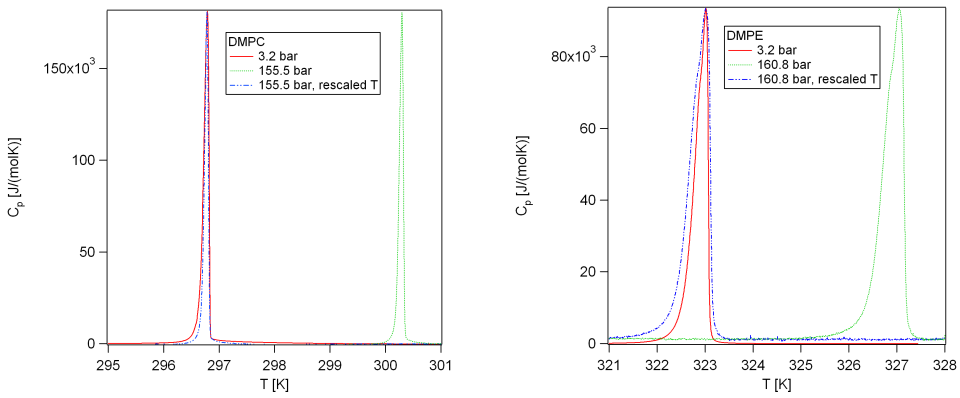

Figure 15: The heat capacity of high pressure samples has been rescaled.

Lipid	Δp bar	$(1+\gamma\Delta p)^{-1}$	γ 10^{-4} ml/J
DLPC	156.9	0.98812	7.67
DMPC	152.3	0.98830	7.77
DPPC	156.0	0.98793	7.83
DSPC	158.3	0.98761	7.93
DMPE	157.6	0.98775	7.87
DPPE	153.5	0.98905	7.22
DMPG	158.0	0.98815	7.59
DPPG	156.8	0.98779	7.88

Table 2: Results of pressure experiments

(like for DMPE in fig. 15) and in some cases a bit narrower.

Using eqn. 15 I have calculated the volume changes. The results are shown in fig. 16. In each case I have used the corresponding value of γ just found.

4.3 Errors

The syringes used for sample preparation have an error of 1%. The weigh used has a precision of $\pm$ 0.0001 g. A typical amount of lipid weighed out is 0.05 g giving an error of 0.2%. An important source of errors is when integrating the heat capacity profiles as have been described previously. The deviation found when doing 10 integrations on the same lipid lied between 2% and 7%. The error made of the DSC is insignificant compared to the other sources of error.

Error sources which are more difficult to put numbers on are for example that some lipid tends to stick to the sides of the container and stay there, when samples were prepared. This of course alters the concentration, which is used in calculation of the enthalpy. A maybe more important concentration error source is that the lipids sink. They are vortexed just before transfer with the syringe but for some of the lipids like for example the PEs the sinking happens very fast.

I had problems with a bubble in the high precision syringe. No matter what was done to avoid it, a bubble came into the syringe during loading. Attention was made to that the bubble stayed in the syringe, when the samples were transferred to the DSC. So the volume put into the DSC should not be affected.

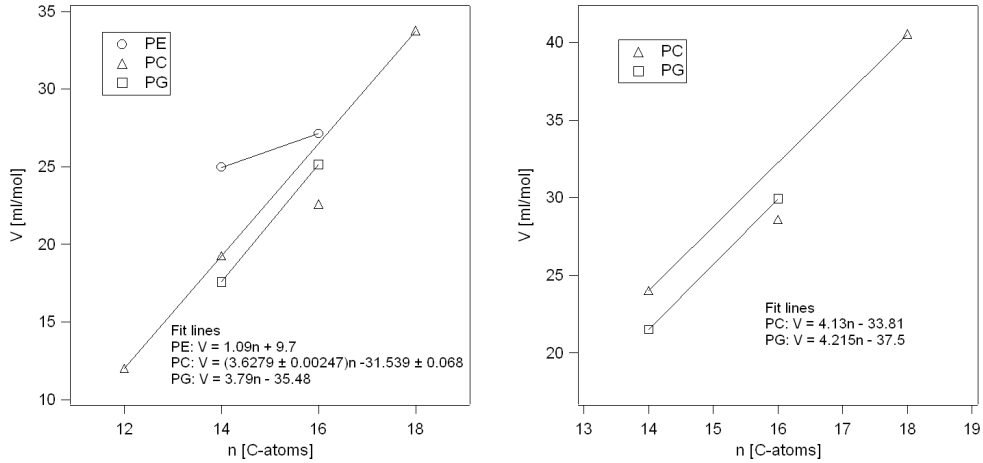

Figure 16: *Left:* Volume changes of the main transition as a function of chain length. *Right:* Volume changes of the main and pretransition as a function of chain length.

One or two scans have been made for each lipid (if the experiment succeeded in the first attempt). Of course even more measurements would have given more convincing results.

4.4 Discussion

The negative heat capacity in the profile of DMPE shown in fig. 13 A indicates the existence of a metastable phase. It is seen from eqn. 22 that negative heat capacity is not possible in equilibrium systems.

In section 2.1.2 I have described how heating scans can give negative enthalpy changes for DLPE if the fluid phase crystallizes. I have not found reports specific on the same behaviour for DMPE but it could be somthing likely that happens. There is however things speaking against it.

For example transition from L_α to L_c is described to happen when the lipid is incubated at the right temperature. This is not done with my sample. I use a low scan rate but the behaviour seen in fig. 13 A is not observed by [28] who uses a lower scan rate than I do.

The peaks seen in C and E coincide with the transition temperature (49°C) described as being from the hydrated gel to fluid phase in [28]. I assume that it is the same transition I see and have used the enthalpies found from these two curves as being the main transition for DMPE. An additional higher temperature peak (53.2°C) ascribed to hydration and melting is also

observed in the same article. It is unclear whether it is the transition from L_c or $L_{c'}$. I get the second transition at 57°C.

When first heated to above the higher transition temperature subsequent heating and cooling only show the lower temperature transition. The second transition is at least only seen in a minor form (*insert*). The phase behaviour seen in A was restored when I made the pressure calorimetry experiment on the same sample 2 months later (data not shown). This is consistent with what is described for the anhydrous phase.

It is also unclear why two peaks are observed in the cooling scans. To figure out exactly what is going on requires further experiments.

DPPE was heated to well above the main transition temperature before measuring the heat capacity and showed a profile similar to that of fig 13 E in the first scan and only one peak in the following.

The submain transition of DSPC and the broad melting regime of DMPG turned up as predicted in the theory section. Addition of salt made the later transition narrower with a minor decrease in enthalpy change. More experiments are required to determine if it is only a deviation.

Fig. 14 shows that the enthalpy changes are indeed related to the of chain length. Looking at the PCs it is seen that there is a clear linear relation between enthalpy and chain length. The enthalpy of DPPC ($n = 16$) is a bit low compared to the line and to literature, where it is given to be 34 ±2 kJ for the main transition [26]. This valued fits nicely in my linear relation.

For PG I get almost the exact same slope as for PC. Taken into account that I only have two points for PE this slope also be assumed to be the same. Therefore the slope can be interpreted as the enthalpy necessary for the transition of two methylene groups (2 CH_2). The number 2 comes because each lipid has 2 hydrocarbon chains. In the same notion the intersection of fit lines with the y-axis could be presumed to be the contribution to the enthalpy change from the head groups.

It has been shown that the heat capacity is always positive (eqn. **??**). Therefore also ΔH_t must be positive as long as $T_1 < T_2$ (cf. eqn. 10). The same can be seen for ΔS_t if eqn. 7 is rewritten as

$$\Delta S_t = \int_{T_1}^{T_2} \frac{c_p}{T} dT \tag{34}$$

.

It has been shown that the transition temperature is related to the changes of enthalpy and entropy by $T_t = \Delta H / \Delta S$ (cf. eqn. 29) So it is seen that a negative ΔH requires either a negative ΔS or T_t. None of which make sense.

Lipid	ΔH_{head} kJ/mol	ΔH_n kJ/mol	n_0
PC main	38.1	4.48	8.5
PE main	9.4	2.94	3.2
PG main	38.2	4.28	8.9
PC pre+main	39.9	3.06	8.0
PG pre+main	39.1	4.82	8.1

Table 3: Results of DSC-experiments. H_{head} is the intersection between the fit line and the y-axis, H_n is the slope of the fit lines and n_0 is the intersection between the fit line and the x-axis. Main and pre+main indicate whether H is taken as an integral over the main or pre- and main transition.

Therefore it can be concluded that for chains shorter than the intersection between the x-axis and the fit lines no transition can take place. The chain length where the fit line intersects is denoted n_0. It is found that the n_0 lies between 8 and 9 with an exception for PE, which gives a value of 3.2. Similar conclusions can be made for volume changes.

An overview of the results obtained from fig. 14 is given in table 3.

The missing correspondence between heat capacity profiles made with and without application of high pressure means that I can not in general verify the proportionality between changes in enthalpy and volume as found by [14]. The bad matches can probably at least partly be ascribed to my lack of experience. Some of the samples have been kept in the freezer for months between the measurements done with ordinary calorimetry and pressure calorimetry. In this time the shape of the vesicles may have changed, which can affect the melting profiles [31]. A shorter time between the two measurements would most likely have helped.

Within error I get the same value of γ for all the lipids. DPPE deviates slightly from the other values but is not significant. This can be seen in table 2 and it is illustrated in fig. 16. In the later I again get a nice linear dependence of chain length by calculating the volume change by the use of the found γ-values.

That γ is the same for all lipids makes it possible to make conclusion not only for single lipid membranes but also for mixed membranes without the need of a detailed knowledge about the composition.

5 Conclusion

The purpose of this thesis was to test if the proportionality between volume and enthalpy changes holds and to find the proportionality constant. This was done by testing a variety of lipids with different head groups and chain lengths. During the testing different characteristics and peculiarities for the different lipids turned up.

Despite their different transitional behaviours common features was also found. I get a very nice linear relation between change in enthalpy and chain length with approximately the same slope for the three different kinds of lipids. Intersections of the fit line with the y-axis and the slope of the fit line give an indication of the contribution of enthalpy change during a transition from the head group and a methylene group respectively. For chain lengths below the intersection between the x-axis and the fit lines it is concluded that no transition can take place.

It is not totally evident from my experiments that the proportional relation between volume and enthalpy changes holds. This is because I do not get an exact match between the two curves made at different pressure. Unfortunately this keeps me from concluding the direct relation between compressibility and heat capacity.

On the other hand if the proportionality exists, as it is shown in [14], I get the same value of γ for all lipids tested. This is very useful if one wants to deduce compressibilitiy of unknown lipid mixtures.

6 Bibliography

References

[1] http://en.wikipedia.org/wiki/Cell_%28biology%29

[2] www.avantilipids.com

[3] V. P. Ivanova (2000) *Theoretical and experimental study of protein-lipid interactions*, Ph.d. thesis, Georg-August-Universität zu Göttingen, pp. 1-23

[4] B. Albert et al (2002) *Molecular biology of The Cell*, pp. 118-119, 583-593, Fourth edition, Garland Science

[5] G. Cevc and D. Marsh (1987) *Phospholipid bilayers: Physical Principles and models*, Wiley

[6] T. Heimburg (2001) *Umwandlungen und Phasenübergänge in biologischen Systemen*, in: Effekte der Physik, M. von Ardenne, G. Musiol, S. Reball (Eds.)

[7] C. Tanford (1978) *The Hydrophobic Effect and the organization of living matter*, Science, New Series, 200, pp. 1012-1018

[8] T. Heimburg and M. Gudmand (2005) *Selvorganisering i Biomembraner*, Kvant, 3-05, 22-24

[9] T. Heimburg and A. D. Jackson (2005) *On soliton propagation in biomembranes and nerves*, PNAS, 102, 9790-9795

[10] D. Marsh (1991) *General features of phospholipids phase transitions*, Chemistry and physics of lipids, 57, 109-120

[11] R. Winter (2005) *Exploring the temperature-pressure configurational landscape of biomolecules: from lipid membranes to proteins*, Philosophical transactions of the royal society A, 363, 537-563

[12] S. Doniac (1978) *Thermodynamic fluctuations in phospholipids bilayers*, Journal of Chemical Physics, 68, 4912-4916

[13] T. Heimburg (2000) *A model for the lipid pretransition: Coupling of ripple formation with the chain-melting transition*, Biophysical Journal, 78, 1154-1165

[14] H. Ebel et al (2001) *Enthalpy and volume changes in lipid membranes. I. The proportionality of heat and volume changes in the lipid melting transition and its implication for the elastic constants*, Journal of Physical Chemistry B, 105, 7353-7360

[15] P. Nissen (2006) *Effects of octanol on the main transition in model lipid membranes*, Bachelor project, University of Copenhagen

[16] B. Mengel and M. Christiansen (2005) *Influence of anaesthetics on the melting transition of lipid membranes*, Bachelor project, University of Copenhagen

[17] M. Kranenburg and B. Smit (2005) *Phase behaviour of model lipid bilayers*, Journal of physical chemistry, 109, 6553-6563

[18] K. Jørgensen (1995) *Calorimetric detection of a sub-main transition in long-chain phosphatidylcholine lipid bilayers*, Biochimica et Biophysica Acta, 1204, 111-114

[19] K. Pressl (1997) *Characterization of the sub-main-transition in distearoylphosphatidylcholine studied by simultaneous small- and wide-angle X-ray diffraction*, Biochimica et Biophysica Acta, 1325, 1-7

[20] M. Nielsen et al (1996) *Model of a sub-main transition in phospholipids bilayers*, Biochimica et biophysica acta, 1283, 170-176

[21] T. McIntosh (1980) *Differences in hydrocarbon tilt between hydrated phosphatidylethanolamine and phosphatidylcholine bilayers. A molecular packing model*, Biophysical Journal, 29, 237-246

[22] M. Kodama and T. Miyata (1996) *Effect of the head group pf phospholipids on the acyl-chain packing and structure of their assemblies as revealed by microcalorimetry and electron microscopy*, Colloids and surfaces A, 109, 283-289

[23] A. Blume (1983) *Apparent Molar Heat Capacities of Phospholipids in Aqueous Dispersion. Effects of Chain Length and Head Group Structure*, Biochemistry, 22, 5436-5442

[24] B. Chowdhry et al (1984) *Multicomponent phase transitions of diacylphosphatidylethanolamine dispersions*, Biophysical Journal, 45, 901-904

[25] S. Mulukutla and G. G. Shipley (1984) *Structure and thermotropic properties of phosphatidylethanolamine and its N-methyl derivatives*, Biochemistry, 23, 2514-2519

[26] A. Blume (1991) *Biological calorimetry: membranes*, Thermochimica Acta, 193, 299-347

[27] J. M. Seddon et al (1983) *Metastability and polymorphism in the gel and fluid bilayer phase of dilauroylphosphatidylethanolamine*, Journal of biological chemistry, 258, 3850-3854

[28] H. H. Mantsch et al (1983) *Studies of the thermotropic behaviour of aqueous phosphatidylethanolamines*, Biochimica et Biophysica Acta, 728, 325-330

[29] M. T. Lamy-Freund and K. A. Riske (2003) *The peculiar thermo-structural behaviour of the anionic lipid DMPG*, Chemistry and Physics of Lipids, 122, 19-32

[30] M. Schneider et al (1999) *Network formation of lipid membranes: Triggering structural transitions by chain melting*, PNAS, 96, 14312-14317

[31] T. Heimburg (2003) *Coupling of chain melting and bilayer structure; domains, rafts elasticity and fusion*, Book chapter in: Planar lipid bilayers (BLMs) and their applications, H.T. Tien & A. Ottova-Leitmannova (Eds.), Elsevier, pp. 269-293

[32] K. A. Riske et al (2004) *Mesoscopic structure in the chain-melting regime of anionic phospholipid vesicles: DMPG*, Biophysical Journal, 86, 3722-3733

[33] C. Kittel and H Kroemer (2002) *Thermal Physics*, second edition, Freeman

[34] T. Heimburg (1998) *Mechanical aspects of membrane thermodynamics. Estimation of mechanical properties of lipid membranes close to the chain melting transition from calorimetry*, Biochimica et Biophysica Acta, 1415, 147-162